

Title Page

Title: The effect of unilateral STN DBS on contralateral STN local field potentials

Running Title: The effect of STN DBS on contralateral STN LFP

Authors & Affiliations:

Harutomo Hasegawa, FRCS¹, Petra Fischer, PhD^{2,3}, Huiling Tan, PhD^{2,3}, Alek Pogosyan, PhD^{2,3}, Michael Samuel, FRCP¹, Peter Brown, PhD^{2,3}, Keyoumars Ashkan, FRCS¹

¹Departments of Neurology and Neurosurgery, King's College Hospital, King's College London, SE5 9RS, London, UK.

²Medical Research Council Brain Network Dynamics Unit at the University of Oxford, OX1 3TH, Oxford, UK.

³Nuffield Department of Clinical Neurosciences, John Radcliffe Hospital, University of Oxford, OX3 9DU, Oxford, UK.

Sources of Financial Support: None

Authorship Statement: We verify that this represents the original work of the authors and that all authors contributed to the conception, design and execution of the study and/or writing of this manuscript.

Conflict of Interest Statement: The authors report no conflicts of interest.

Corresponding Author:

Harutomo Hasegawa, FRCS

Department of Neurosurgery, King's College Hospital, Denmark Hill, London, SE5 9RS

Tel: +44 7765475012 E-mail: h.hasegawa@nhs.net

Abstract

Objectives

Unilateral STN DBS for Parkinson's disease (PD) improves ipsilateral symptoms, but how this occurs is not well understood. We investigated if unilateral STN DBS suppresses contralateral STN beta activity in the local field potential (LFP), since previous research has shown that activity in the beta band can correlate with the severity of contralateral clinical symptoms and is modulated by DBS.

Methods

We recorded STN LFPs from 14 patients who underwent bilateral STN DBS for PD. Following a baseline recording, unilateral STN stimulation was delivered at therapeutic parameters whilst LFPs were recorded from the contralateral (unstimulated) STN.

Results

Unilateral STN DBS suppressed contralateral beta power ($p = 0.039$, relative suppression = $-5.7\% \pm (\text{SD}) 16\%$ when averaging across the highest beta peak channels; $p = 0.033$, relative suppression = $-5.2\% \pm 13\%$ when averaging across all channels). Unilateral STN DBS produced a 17% ipsilateral ($p=0.016$) and 29% contralateral ($p=0.002$) improvement in upper limb hemi-body bradykinesia-rigidity (UPDRS-III, items 3.3-3.6). The ipsilateral clinical improvement and the change in contralateral beta power were not significantly correlated.

Conclusions

Unilateral STN DBS suppresses contralateral STN beta LFP. This indicates that unilateral STN DBS modulates bilateral basal ganglia networks. It remains unclear whether this mechanism accounts for the ipsilateral motor improvements.

Introduction

Unilateral STN DBS for Parkinson's disease improves ipsilateral symptoms¹⁻⁴, but how this occurs is not well understood. The effect of unilateral STN stimulation on the contralateral STN has been studied in patients undergoing STN implantation after the other side has already been implanted⁵⁻⁸. The results are mixed, showing increases^{5,6} and decreases^{7,8} in single⁶⁻⁸ and multi-unit⁵ activity in the contralateral STN. One study showed a reduction in contralateral beta oscillations from single unit recordings in a subset of recordings⁸.

Local field potential (LFP) recordings from the STN have shown that activity in the beta band can correlate with the severity of contralateral clinical symptoms in Parkinson's disease and is modulated by DBS^{9,10}. We therefore hypothesise that the effect of STN DBS on ipsilateral symptoms might be due to suppression of beta activity in the STN contralateral to stimulation. As previous studies of DBS induced changes in contralateral STN have not explicitly explored changes in the LFP we sought to study the effect of unilateral STN DBS on contralateral STN LFPs in patients who have undergone bilateral STN DBS.

Methods

We studied 14 patients (28 STN sides) who underwent bilateral STN DBS using MRI guided targeting and Medtronic 3389 electrodes at King's College Hospital, London (Table 1)¹¹. The study was approved by the local ethics committee and all patients provided informed consent. The electrode positions were confirmed postoperatively by CT/MRI fusion¹². At least one contact in bipolar recordings was positioned within the STN itself or within 2mm of the STN. Recordings were obtained from externalised electrodes 4-6 days after surgery and after overnight withdrawal of medication. LFPs were amplified, low-pass filtered at 550 Hz,

sampled at 2048Hz, common average referenced and recorded with a TMSi Porti amplifier (TMS International, Netherlands). The baseline consisted of a 2-minute recording from both STN and separate clinical examination of the upper limbs (UPDRS-III, upper limb bradykinesia-rigidity items 3.3-3.6). Following this, bipolar stimulation was delivered at 130Hz and 60us (N-vision, Medtronic) while LFPs were recorded from the contralateral side. The cathode/anode combination and voltage used for each patient were those that produced optimal clinical improvement in a previous testing session (Table 1). The recording at rest was stopped after 12 minutes of stimulation and the clinical assessment was repeated whilst stimulation continued. The sides were switched and the same procedure repeated after a 10 minute washout period.

Data pre-processing

All spectral analyses were performed in MATLAB (RRID:SCR_001622, v. 2016a, The MathWorks Inc., Natick, Massachusetts). Spatially focal bipolar signals were computed off-line by subtracting the data from two adjacent electrode contacts¹³. Data were high-pass filtered (*fieldtrip*-function *ft_preproc_highpassfilter*¹⁴, 1Hz cut-off, Butterworth filter, filter order = 4, passed forwards and backwards) and artefacts were excluded upon visual inspection ($2.5 \pm 4.2\%$ data points were excluded). To match the data length between the recordings, only the final two minutes of each stimulation recording were analysed.

Spectral analyses

After z-scoring and down-sampling the data to 200Hz, the power spectral density between 5-45Hz (with a 0.5Hz resolution) was estimated using Welch's method (MATLAB function *pwelch*, overlap = 0.5, 2s hamming window). This method calculates the power by computing

the discrete Fourier transform in overlapping windows and then averages across resulting spectra to attenuate peaks due to noise. The resulting spectra were smoothed with a 3Hz-wide moving average (MATLAB function *smooth*) to reduce sharp bumps in the spectra. Data from five electrodes (P3 Le, P4 Le, P10 Le, P12 Le, P13 Ri) and from three bipolar channels of two electrodes (P3: R2R3, P12: L1L2, L2L3) had to be excluded because the spectra in the STIM_OFF and STIM_ON condition showed strong offsets across the 5-45Hz band consistent with elevated noise levels secondary to contamination with stimulation artefacts. This resulted in 66 bipolar signals from 23 electrodes that were analysed.

Detection of the bipolar signal with the strongest beta peak

Because past research has linked maximal beta band activity to the dorsal (motor) region of the STN¹⁵⁻¹⁷, which also corresponds to the site that offers the most effective stimulation^{16,18,19}, we wanted to test if beta suppression is particularly pronounced in the region that exhibits the strongest beta peak. We therefore selected the bipolar contact pair with the highest amplitude in the beta band (detected after log-log transforming the spectra and subtracting the linear trend fitted with a robust regression using the MATLAB function *robustfit*) and averaged the beta power at this across electrodes, as well as averaging the beta power across all contact pairs before averaging across electrodes.

Statistical testing

Statistical tests were performed on the average across all bipolar signals, as well as on the bipolar signals that showed the highest beta peak and the signals obtained from the contacts that were used for stimulation. Pairwise comparisons of average beta power (13-30 Hz) between the ON_STIM and OFF_STIM condition and clinical data were analysed with t-tests

or nonparametric Wilcoxon signed-rank tests if Lilliefors tests showed that the data were not normal distributed. Where t-tests were computed, the t-statistics are reported after the p-value. 95% bootstrapped confidence intervals of the mean beta power difference across subjects were computed using the MATLAB function *bootci* (using 2000 samples). Note that for one comparison the confidence limits (CLs) included zero despite the p-value calculated with a non-parametric Wilcoxon-signed rank test being below 0.05. This can happen because bootstrapped CLs take the skewness of a distribution into account while the non-parametric test is based on ranking the data, giving less weight to the extent of the differences.

Multiple-comparison correction for power differences across multiple frequency bins was performed by using a cluster-based permutation correction approach²⁰. The condition labels were randomly permuted 2000 times such that each data pair was maintained but its order of subtraction might change (resulting in a change in sign for this pair) to create a null-hypothesis distribution. Suprathreshold-clusters (pre-cluster threshold: $P < 0.05$) were obtained for the original unpermuted data and for each permutation sample by computing the z-scores relative to the permutation distribution. If the absolute sum of the z-scores within the original suprathreshold-clusters exceeded the 95th percentile of the 2000 largest absolute sums of z-scores from the permutation distribution, it was considered statistically significant.

Correlations between spectral and clinical measures were performed with Spearman's correlation.

Results

LFP

The power spectra show beta power (13-30 Hz) suppression during stimulation of the contralateral STN (**Figure 1**). The suppression was apparent when averaging across the

spectra from un-normalised signals recorded from all the contacts of each electrode (top left panel, Wilcoxon-signed rank test, $n=23$, $p = 0.033$, relative suppression = $-5.2\% \pm$ (SD) 13% , bootstrapped 95% CIs = $[-10.7\%, -0.6\%]$). A number of further exploratory analyses were performed to test the robustness of this finding. Averaging across the highest beta peak channels (top middle panel, Wilcoxon-signed rank test, $n = 23$, $p = 0.039$, relative suppression = $-5.7\% \pm 16\%$, CIs = $[-12\%, 0.5\%]$) and across the bipolar contacts used for stimulation (top right panel, $p = 0.101$, relative suppression = $-5.9\% \pm 13.3\%$, CIs = $[-11.6\%, -0.8\%]$) also revealed beta power suppression. In addition, significant beta power suppression was evident when normalizing the power spectra relative to the 5-45 Hz power average taken across both the baseline and the stimulation condition (middle panels; Wilcoxon-signed rank tests, $n = 23$, average over all channels: $p = 0.042$, relative suppression = $-6.9\% \pm 16\%$, CIs = $[-15.3\% -2.0\%]$; highest beta peak channels: $p = 0.042$, relative suppression = $-8.7\% \pm 20\%$, CIs = $[-18.2\% -2.1\%]$; bipolar contacts used for stimulation: $p = 0.024$, $t_{22} = -2.4$, relative suppression = $-6.7\% \pm 13.3$, CIs = $[-13.0\% -2.1\%]$).

Note that the strength of relative suppression had a large variability relative to the effect size, partly because three recordings, which did not show a distinct beta peak, were also included in the analyses. The variability is illustrated by the confidence limits specified above and illustrated in the top and middle panels of Fig 1, and in the individual results given in the lower panels of the same figure. The effects were increased if the sides without a clear beta peak were excluded (Wilcoxon-signed rank tests, $n = 20$; un-normalised: average over all channels: $p = 0.014$, relative suppression = $-6.8\% \pm 12.6\%$, CIs = $[-12.5\% -1.9\%]$; highest beta peak channels: $p = 0.017$, relative suppression = $-7.7\% \pm 16.3\%$, CIs = $[-14.7\% -0.6\%]$; bipolar contacts used for stimulation: $p = 0.026$, $t_{19}=-2.4$, relative suppression = $-8.1\% \pm 12.6\%$, CIs = $[-13.6\% -2.7\%]$; normalised to total power: average over all channels: $p = 0.011$,

relative suppression = $-8.6\% \pm 16.2\%$, CIs = $[-17.2\% -3.0\%]$; highest beta peak channels: $p = 0.012$, relative suppression = $-11.1\% \pm 20.7\%$, CIs = $[-22.2\% -3.8\%]$; bipolar contacts used for stimulation: $p = 0.009$, $t_{19} = -2.9$, relative suppression = $-8.6\% \pm 13.2\%$, CIs = $[-14.9\% - 3.3\%]$).

Clinical

Two patients did not tolerate the clinical testing (P3 and P4) and one patient tolerated testing on one side only (P6). The mean baseline UPDRS score, including both the left and right sides, was 6.1. Unilateral STN stimulation produced a 17% ipsilateral (Wilcoxon-signed rank test, $n = 23$, $p=0.016$) and 29% contralateral (Wilcoxon-signed rank test, $n = 23$, $p=0.002$) improvement in upper limb hemi-body UPDRS. There was a significant difference between the ipsilateral and contralateral clinical change (Wilcoxon-signed rank test, $p=0.015$). The clinical improvement and the change in beta power were not significantly correlated (**Figure 2**).

Discussion

Since beta LFP activity is exaggerated in Parkinson's disease and its suppression by DBS improves with clinical symptoms^{9,10}, a reduction in contralateral beta LFP following unilateral stimulation could mediate ipsilateral clinical improvement. However, the degree of beta suppression in the STN contralateral to the stimulated STN was small, ranging from about 5 to 11% depending on how it was estimated. Whitmer et al. (2012) and Eusebio et al. (2011) reported a suppression of beta activity during simultaneous recording and stimulation of the same STN of 47% and 54%, respectively^{9,21}. These suppressions are much greater than

the changes in the contralateral STN reported here, although it should be noted that earlier reports that included a significant number of STN without beta peaks estimated much smaller changes during simultaneous recording and stimulation of the same STN^{22,23}. Although there was a significant improvement in ipsilateral clinical symptoms in our cohort, contralateral beta LFP changes and ipsilateral clinical change were not significantly correlated. This may be due to a variety of factors, including the variability in the spectra across patients and the variable clinical response to STN DBS in the early postoperative period.

The clinical assessor was not blinded to the stimulation side, which may have introduced bias. Our clinical results are however, broadly similar to those reported for double-blinded assessments for contralateral and ipsilateral STN stimulation^{1,3,4}.

This study adds to the literature demonstrating that unilateral intervention in the basal ganglia produces changes in the contralateral basal ganglia^{8,24-27}. The functional anatomy of the basal ganglia incorporates the brainstem and thalamic nuclei, the hypothalamus, limbic system and cerebral cortex^{28,29}. The mechanism by which the contralateral beta LFP is modulated is unknown, although STN-STN connections³⁰ and other indirect crossed pathways may be relevant³¹⁻³⁴. The observation that unilateral subthalamotomy leads to bilateral clinical improvement^{35,36} also suggests that the basal ganglia on the two sides are functionally coupled, and supports the hypothesis that changes in the contralateral STN are probably due to cross-hemispheric pathways rather than volume-conducted spread of stimulation³⁷.

In contrast to microelectrode recordings, LFPs likely reflect synchronous changes in the input to a population of neurons³⁸. Showing that such activity is modulated on the contralateral side to stimulation suggests that DBS is capable of modulating specific networks that mediate

neural synchrony in the opposite hemisphere⁸. It has been proposed that DBS may work by directly disrupting pathological synchronization^{10,39}. Our findings call for an explanation of how this occurs in the contralateral hemisphere, and raise the possibility that DBS may modulate neural networks in the ipsilateral hemisphere.

The effect of unilateral stimulation on contralateral beta LFP shown in this study is similar in frequency to the effect observed in the stimulated STN¹⁰. However, previous work has shown that unilateral dopaminergic lesions of the substantia nigra²⁷ and chemical activation or inhibition of the thalamic parafascicular nucleus⁴⁰, which have direct projections to the contralateral STN, have opposite effects on firing rates in the ipsilateral and contralateral STN. These observations highlight the complexity of cross-hemispheric basal ganglia interactions at single neuron and population levels and the need for further studies to guide neuromodulation approaches.

Unilateral STN DBS has sometimes been performed in preference to bilateral STN DBS when symptoms are predominantly lateralised, with the opposite side being implanted at a later date if required⁴¹. If the anatomical basis of the contralateral effect can be better understood, the question arises as to whether the targeting of unilateral DBS can be optimised to enhance the ipsilateral effect to reduce or delay the need for bilateral implantation⁴².

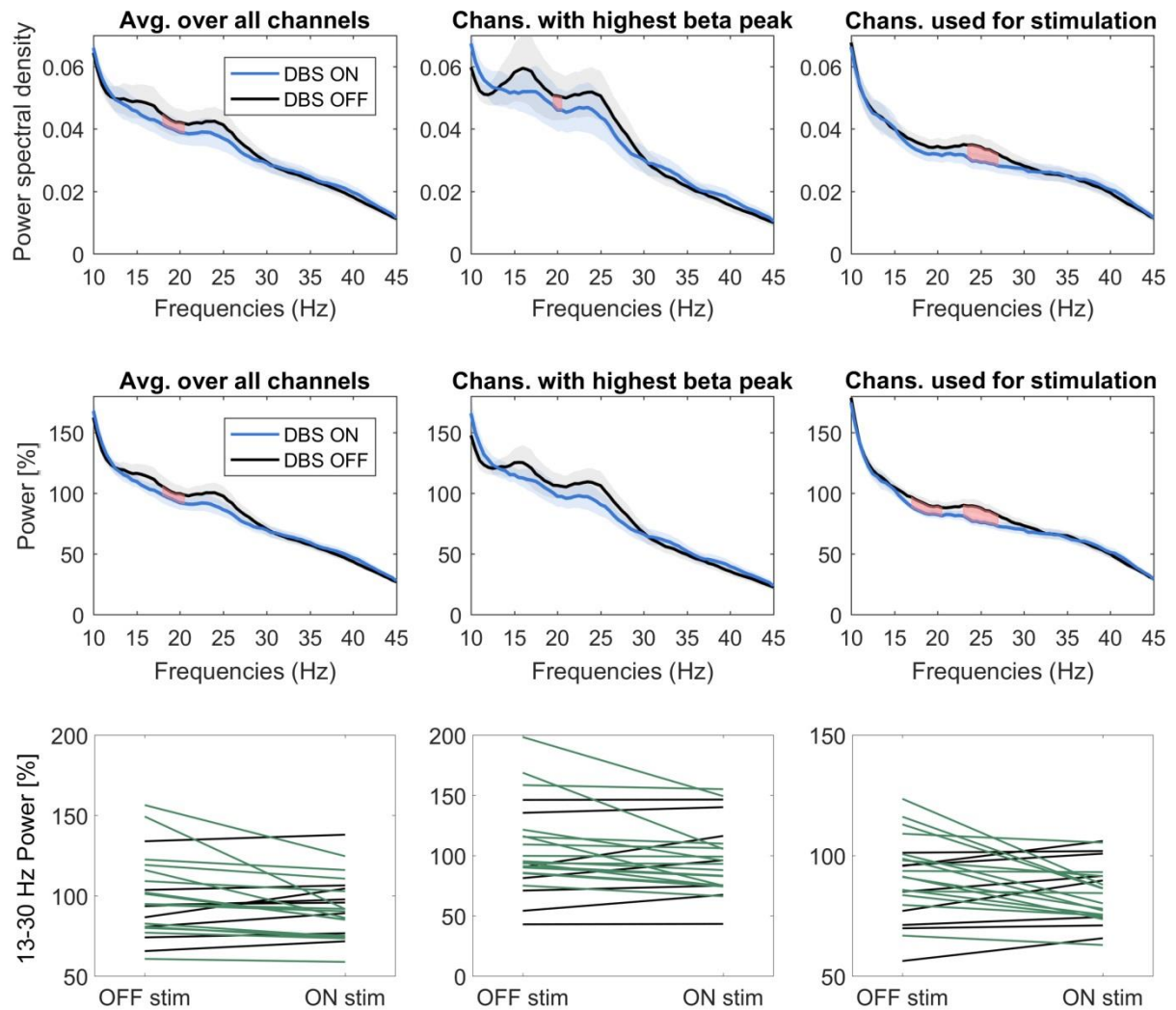
Acknowledgements

This work was supported by the Medical Research Council [MC_UU_12024/1]. PB was further funded by the National Institute of Health Research Oxford Biomedical Research Centre.

Table 1: Patient characteristics

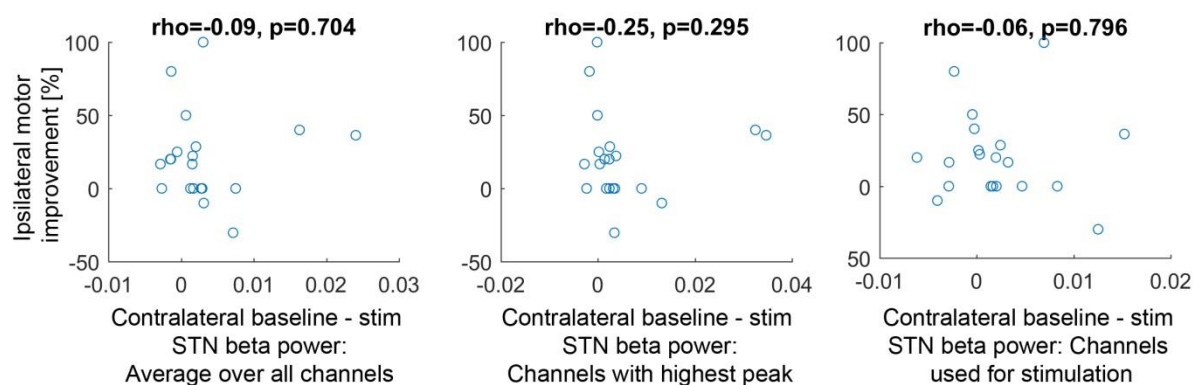
| Patient | Sex | Age | Handedness | Disease Duration (years) | Symptom side | Symptoms | Pre-op UPDRS off/on | Left Stim | Right Stim |
|---------|-----|-----|------------|--------------------------|--------------|--|---------------------|-----------------|-----------------|
| 1 | M | 74 | R | 16 | Both (R>L) | Right hand tremor, right leg tremor, jaw tremor, left arm tremor, bradykinesia, rigidity | 30/5.5 | 0-, 1+, 1V | 0-, 1+, 1V |
| 2 | M | 58 | R | 7 | Both (R>L) | Right hand tremor, right leg tremor, dyskinesia, fluctuations | 41/12 | 0-, 1+, 2.5V | 0-, 1+, 1V |
| 3 | M | 57 | R | 6 | Both (R>L) | Right hand tremor, off symptoms, fluctuations, freezing | 14/4.5 | 0-, 1+, 2V | 0-, 1+, 2V |
| 4 | M | 68 | R | 12 | Both | Freezing, fluctuations, dyskinesia | 40/17 | 0-, 1+, 2V | 0-, 1+, 3V |
| 5 | M | 61 | R | 11 | Both | Tremor, dyskinesia | 53/26 | 0-, 1+, 2.5V | 0-, 1+, 2.5V |
| 6 | M | 65 | R | 10 | Both | Tremor, bradykinesia, freezing | 37/9 | 0-, 1+, 1.5V | 0-, 1+, 1.5V |
| 7 | F | 70 | R | 20 | Both | Tremor, rigidity, bradykinesia, dyskinesia | 54/19 | 0-, 1+, 2.5V | 0-, 1+, 2.5V |
| 8 | M | 69 | R | 17 | Both | Tremor, bradykinesia, rigidity, camptocomia, dyskinesia | 37/18.5 | 0-, 1+, 2.5V | 0-, 1+, 2.5V |
| 9 | M | 72 | R | 5 | Both | Tremor, bradykinesia | 41/23.5 | 0-, 1+, 2.5V | 0-, 1+, 2.5V |
| 10 | F | 75 | R | 7 | Both | Tremor, bradykinesia, freezing | 36/19 | 1-, 2+, 2V | 0-, 1+, 2V |
| 11 | M | 54 | R | 8 | Both | Tremor, bradykinesia, rigidity | 29.5/5 | 0-, 1+, 2V | 0-, 1+, 2V |
| 12 | M | 59 | R | 6 | Both | Rigidity, bradykinesia, tremor | 46/8 | 1-, 2+, 2V | 0-, 1+, 2V |
| 13 | M | 71 | R | 15 | Both (R>L) | Tremor, rigidity, bradykinesia | 12/4 | 0-, 1+, 2.5V | 0-, 1+, 2.5V |
| 14 | M | 65 | R | 9 | Both | Tremor, dyskinesia, off-dystonia | 26/9.5 | 0-, 1+, 2V | 0-, 1+, 2V |

Figure 1



Beta power suppression with contralateral DBS. The panels in the left column show the average power spectral density (top) and relative power change (middle and bottom) of all bipolar signals without preselecting any channels. The panels in the middle column show the average across the 23 bipolar signals with the highest beta peak from each electrode. The panels in the right column show the average of the 23 bipolar signals corresponding to the contacts used for stimulation. Shaded areas show the standard error of the mean. Green lines show recordings where beta power decreased when the stimulation was on, black lines show recordings where it increased.

Figure 2



Scatter plots showing the correlations between the improvement of the bradykinesia UPDRS scores obtained ipsilateral to the stimulated STN and the beta power suppression occurring with contralateral stimulation relative to the baseline recording. The titles show the Spearman's correlation coefficients, which were not significant. Improvement is positive on the y-axis, and baseline-stimulation STN beta power (on the x-axis) is also positive if beta was suppressed on stimulation. The x-axis on the left panel shows the average 13-30 Hz difference of all bipolar signals without pre-selecting any channels. The x-axis on the middle panel shows the 13-30 Hz difference from the bipolar signals that showed the highest beta peak (one per electrode). The x-axis on the right panel shows the 13-30 Hz difference of the bipolar signals corresponding to the contacts used for stimulation. Only 20 recordings are shown as the patients did not tolerate the UPDRS testing in three recordings.

References

1. Tabbal SD, Ushe M, Mink JW, et al. Unilateral subthalamic nucleus stimulation has a measurable ipsilateral effect on rigidity and bradykinesia in Parkinson disease. *Exp Neurol*. 2008;211(1):234-242.
2. Chung SJ, Jeon SR, Kim SR, Sung YH, Lee MC. Bilateral effects of unilateral subthalamic nucleus deep brain stimulation in advanced Parkinson's disease. *European neurology*. 2006;56(2):127-132.
3. Walker HC, Watts RL, Guthrie S, Wang D, Guthrie BL. Bilateral effects of unilateral subthalamic deep brain stimulation on Parkinson's disease at 1 year. *Neurosurgery*. 2009;65(2):302-309; discussion 309-310.
4. Germano IM, Gracies JM, Weisz DJ, Tse W, Koller WC, Olanow CW. Unilateral stimulation of the subthalamic nucleus in Parkinson disease: a double-blind 12-month evaluation study. *Journal of neurosurgery*. 2004;101(1):36-42.
5. Novak P, Klemp JA, Ridings LW, Lyons KE, Pahwa R, Nazzaro JM. Effect of deep brain stimulation of the subthalamic nucleus upon the contralateral subthalamic nucleus in Parkinson disease. *Neuroscience letters*. 2009;463(1):12-16.
6. Walker HC, Watts RL, Schrandt CJ, et al. Activation of subthalamic neurons by contralateral subthalamic deep brain stimulation in Parkinson disease. *J Neurophysiol*. 2011;105(3):1112-1121.
7. Toleikis JR, Metman LV, Pilitsis JG, Barborica A, Toleikis SC, Bakay RA. Effect of intraoperative subthalamic nucleus DBS on human single-unit activity in the ipsilateral and contralateral subthalamic nucleus. *Journal of neurosurgery*. 2012;116(5):1134-1143.

8. Brun Y, Karachi C, Fernandez-Vidal S, et al. Does unilateral basal ganglia activity functionally influence the contralateral side? What we can learn from STN stimulation in patients with Parkinson's disease. *J Neurophysiol.* 2012;108(6):1575-1583.
9. Eusebio A, Thevathasan W, Doyle Gaynor L, et al. Deep brain stimulation can suppress pathological synchronisation in parkinsonian patients. *Journal of neurology, neurosurgery, and psychiatry.* 2011;82(5):569-573.
10. Kuhn AA, Kempf F, Brucke C, et al. High-frequency stimulation of the subthalamic nucleus suppresses oscillatory beta activity in patients with Parkinson's disease in parallel with improvement in motor performance. *J Neurosci.* 2008;28(24):6165-6173.
11. Ashkan K, Blomstedt P, Zrinzo L, et al. Variability of the subthalamic nucleus: the case for direct MRI guided targeting. *British journal of neurosurgery.* 2007;21(2):197-200.
12. Ellenbogen JR, Tuura R, Ashkan K. Localisation of DBS Electrodes Post-Implantation, to CT or MRI? Which Is the Best Option? *Stereotactic and functional neurosurgery.* 2018;96(5):347-348.
13. Marmor O, Valsky D, Joshua M, et al. Local vs. volume conductance activity of field potentials in the human subthalamic nucleus. *Journal of neurophysiology.* 2017;117(6):2140-2151.
14. Oostenveld R, Fries P, Maris E, Schoffelen JM. FieldTrip: Open source software for advanced analysis of MEG, EEG, and invasive electrophysiological data. *Computational intelligence and neuroscience.* 2011;2011:156869.
15. Chen CC, Pogosyan A, Zrinzo LU, et al. Intra-operative recordings of local field potentials can help localize the subthalamic nucleus in Parkinson's disease surgery. *Exp Neurol.* 2006;198(1):214-221.
16. Zaidel A, Spivak A, Grieb B, Bergman H, Israel Z. Subthalamic span of beta oscillations predicts deep brain stimulation efficacy for patients with Parkinson's disease. *Brain.* 2010;133(Pt 7):2007-2021.
17. Horn A, Neumann WJ, Degen K, Schneider GH, Kuhn AA. Toward an electrophysiological "sweet spot" for deep brain stimulation in the subthalamic nucleus. *Hum Brain Mapp.* 2017;38(7):3377-3390.
18. Ince NF, Gupte A, Wichmann T, et al. Selection of optimal programming contacts based on local field potential recordings from subthalamic nucleus in patients with Parkinson's disease. *Neurosurgery.* 2010;67(2):390-397.
19. Tinkhauser G, Pogosyan A, Debove I, et al. Directional local field potentials: A tool to optimize deep brain stimulation. *Mov Disord.* 2018;33(1):159-164.
20. Maris E, Oostenveld R. Nonparametric statistical testing of EEG- and MEG-data. *Journal of neuroscience methods.* 2007;164(1):177-190.
21. Whitmer D, de Solages C, Hill B, Yu H, Henderson JM, Bronte-Stewart H. High frequency deep brain stimulation attenuates subthalamic and cortical rhythms in Parkinson's disease. *Frontiers in human neuroscience.* 2012;6:155.
22. Rossi L, Marceglia S, Foffani G, et al. Subthalamic local field potential oscillations during ongoing deep brain stimulation in Parkinson's disease. *Brain research bulletin.* 2008;76(5):512-521.
23. Giannicola G, Marceglia S, Rossi L, et al. The effects of levodopa and ongoing deep brain stimulation on subthalamic beta oscillations in Parkinson's disease. *Exp Neurol.* 2010;226(1):120-127.
24. Arai N, Yokochi F, Ohnishi T, et al. Mechanisms of unilateral STN-DBS in patients with Parkinson's disease : a PET study. *Journal of neurology.* 2008;255(8):1236-1243.

25. Liu X, Ford-Dunn HL, Hayward GN, et al. The oscillatory activity in the Parkinsonian subthalamic nucleus investigated using the macro-electrodes for deep brain stimulation. *Clinical neurophysiology : official journal of the International Federation of Clinical Neurophysiology*. 2002;113(11):1667-1672.
26. Neagu B, Tsang E, Mazzella F, et al. Pedunculopontine nucleus evoked potentials from subthalamic nucleus stimulation in Parkinson's disease. *Exp Neurol*. 2013;250:221-227.
27. Perier C, Agid Y, Hirsch EC, Feger J. Ipsilateral and contralateral subthalamic activity after unilateral dopaminergic lesion. *Neuroreport*. 2000;11(14):3275-3278.
28. Eid L, Parent M. Chemical anatomy of pallidal afferents in primates. *Brain Struct Funct*. 2016;221(9):4291-4317.
29. Parent A, Hazrati LN. Functional anatomy of the basal ganglia. II. The place of subthalamic nucleus and external pallidum in basal ganglia circuitry. *Brain Res Rev*. 1995;20:128-154.
30. Cavdar S, Ozgur M, Cakmak YO, Kuvvet Y, Kunt SK, Saglam G. Afferent projections of the subthalamic nucleus in the rat: emphasis on bilateral and interhemispheric connections. *Acta neurobiologiae experimentalis*. 2018;78(3):251-263.
31. Castle M, Aymerich MS, Sanchez-Escobar C, Gonzalo N, Obeso JA, Lanciego JL. Thalamic innervation of the direct and indirect basal ganglia pathways in the rat: Ipsi- and contralateral projections. *The Journal of comparative neurology*. 2005;483(2):143-153.
32. Hazrati LN, Parent A. Contralateral pallidothalamic and pallidotegmental projections in primates: an anterograde and retrograde labeling study. *Brain Res*. 1991;567(2):212-223.
33. Parent M, Parent A. The microcircuitry of primate subthalamic nucleus. *Parkinsonism & related disorders*. 2007;13 Suppl 3:S292-295.
34. Castrioto A, Meaney C, Hamani C, et al. The dominant-STN phenomenon in bilateral STN DBS for Parkinson's disease. *Neurobiology of disease*. 2011;41(1):131-137.
35. Alvarez L, Macias R, Guridi J, et al. Dorsal subthalamotomy for Parkinson's disease. *Mov Disord*. 2001;16(1):72-78.
36. Aziz TZ, Peggs D, Sambrook MA, Crossman AR. Lesion of the subthalamic nucleus for the alleviation of 1-methyl-4-phenyl-1,2,3,6-tetrahydropyridine (MPTP)-induced parkinsonism in the primate. *Mov Disord*. 1991;6(4):288-292.
37. Miocinovic S, Lempka SF, Russo GS, et al. Experimental and theoretical characterization of the voltage distribution generated by deep brain stimulation. *Exp Neurol*. 2009;216(1):166-176.
38. Buzsaki G, Anastassiou CA, Koch C. The origin of extracellular fields and currents--EEG, ECoG, LFP and spikes. *Nat Rev Neurosci*. 2012;13(6):407-420.
39. McConnell GC, So RQ, Grill WM. Failure to suppress low-frequency neuronal oscillatory activity underlies the reduced effectiveness of random patterns of deep brain stimulation. *Journal of neurophysiology*. 2016;115(6):2791-2802.
40. Mouroux M, Hassani OK, Feger J. Electrophysiological study of the excitatory parafascicular projection to the subthalamic nucleus and evidence for ipsi- and contralateral controls. *Neuroscience*. 1995;67(2):399-407.
41. Taba HA, Wu SS, Foote KD, et al. A closer look at unilateral versus bilateral deep brain stimulation: results of the National Institutes of Health COMPARE cohort. *Journal of neurosurgery*. 2010;113(6):1224-1229.
42. Shenai MB, Romeo A, Walker HC, Guthrie S, Watts RL, Guthrie BL. Spatial topographies of unilateral subthalamic nucleus deep brain stimulation efficacy for

ipsilateral, contralateral, midline, and total Parkinson disease motor symptoms.
Neurosurgery. 2015;11 Suppl 2:80-88; discussion 88.